First publ. in: European Journal of Cell Biology 88 (2009), 1, pp. 45–63

Immunolocalisation of PrP^{Sc} in scrapie-infected N2a mouse neuroblastoma cells by light and electron microscopy

Nathalie M. Veith[a], Helmut Plattner[b,*], Claudia A.O. Stuermer[c], Walter J. Schulz-Schaeffer[d], Alexander Bürkle[a,*]

[a]*Molecular Toxicology, Department of Biology, University of Konstanz, Box X911, D-78457 Konstanz, Germany*
[b]*Cell Biology, Department of Biology, University of Konstanz, Konstanz, Germany*
[c]*Developmental Neurobiology, Department of Biology, University of Konstanz, Konstanz, Germany*
[d]*Prion and Dementia Research Unit, Institute of Neuropathology, University of Göttingen, Göttingen, Germany*

Abstract

The causative agent of transmissible spongiform encephalopathies (TSE) is PrP^{Sc}, an infectious, misfolded isoform of the cellular prion protein (PrP^{C}). The localisation and trafficking of PrP^{Sc} and sites of conversion from PrP^{C} to PrP^{Sc} are under debate, particularly since most published work did not discriminate between PrP^{C} and PrP^{Sc}. Here we describe the localisation of PrP^{C} and PrP^{Sc} in a scrapie-infected neuroblastoma cell line, ScN2a, by light and electron microscopic immunolocalisation. After eliminating PrP^{C} with proteinase K, PrP^{Sc} was detected at the plasma membrane, endocytosed via clathrin-coated pits and delivered to early endosomes. Finally, PrP^{Sc} was detected in late endosomes/lysosomes. As we detected PrP^{Sc} at the cell surface, in early endosomes and in late endosomes/lysosomes, i.e. locations where PrP^{C} is also present, our data imply that the conversion process could take place at the plasma membrane and/or along the endocytic pathway. Finally, we observed the release of PrP^{C}/PrP^{Sc} via exocytotic pathways, i.e. via exosomes and as an opaque electron-dense mass which may represent a mechanism of intercellular spreading of infectious prions.

Keywords: PrP^{Sc}; Electron microscopy; Immunofluorescence; Early endosomes; Late endosomes; Lysosomes; Clathrin-coated pits; Exosomes

Introduction

Transmissible spongiform encephalopathies (TSE) are rare, progressive and fatal neurodegenerative disorders of the central nervous system and include scrapie in sheep, bovine spongiform encephalopathy (BSE) in cattle, and sporadic and variant Creutzfeldt-Jakob disease (sCJD and vCJD) in humans (Prusiner, 2001; Unterberger et al., 2005; Tatzelt and Schatzl, 2007; Wadsworth and Collinge, 2007). The brains of affected individuals show spongiform changes, loss of neurons and gliosis. The disease leads to progressive dementia, ataxia and finally death, paralleled by the conversion of the endogenous cellular prion protein (PrP^{C}) into the infectious scrapie form (PrP^{Sc}). In contrast to PrP^{C},

*Corresponding authors. Tel.: +49 7531 884035; fax: +49 7531 884033.
E-mail addresses: helmut.plattner@uni-konstanz.de (H. Plattner), alexander.buerkle@uni-konstanz.de (A. Bürkle).

PrP^{Sc} shows a high content of β-sheet structure, is insoluble in mild detergents, displays a strong tendency to aggregate into amyloid fibrils, and is partially resistant to proteases, e.g. proteinase K (PK) (Taraboulos et al., 1990; Caughey and Baron, 2006).

A number of studies have analysed the trafficking of PrP^{C} in cultured cells. PrP^{C} is synthesised in the endoplasmic reticulum (ER) and travels through the Golgi apparatus to the plasma membrane. There, it is attached via a glycosylphosphatidylinositol (GPI) anchor and assembled in regions exhibiting a specific lipid composition (so-called "rafts") (Taraboulos et al., 1995; Madore et al., 1999; Naslavsky et al., 1999). PrP^{C} can be constitutively internalised. A major pathway for internalisation of PrP^{C} appears to use clathrin-mediated endocytosis, but endocytosis via non-clathrin-coated vesicles (Frick et al., 2007) and so-called "caveolae-like structures" has also been reported (Vey et al., 1996). Some PrP^{C} is recycled back to the cell surface, while the majority is transported through early and late endosomes before it enters lysosomes for degradation (Magalhaes et al., 2002; Sunyach et al., 2003; Prado et al., 2004; Campana et al., 2005).

In contrast to PrP^{C}, the trafficking of PrP^{Sc} is less well described. This relates to the fact that the site of conversion of PrP^{C} to PrP^{Sc} has not been identified. Several studies indicate that PrP^{Sc} is formed after PrP^{C} has reached the plasma membrane (Caughey and Raymond, 1991; Borchelt et al., 1992; Taraboulos et al., 1992; Gilch et al., 2001) or after PrP^{C} internalisation into the endo-/lysosomal compartments (Caughey and Raymond, 1991; Borchelt et al., 1992; Taraboulos et al., 1992; Prado et al., 2004). In fact, formation of PrP^{Sc} is inhibited by blocking endocytosis of PrP^{C} (Borchelt et al., 1992). Moreover, PrP^{Sc} can be cleaved at its N-terminus by endogenous proteases in acidic compartments immediately after its generation (Caughey et al., 1991; Borchelt et al., 1992), but PrP^{Sc} is not completely degraded in lysosomes (Caughey et al., 1991). Its conversion to a protease-resistant state is likely to occur prior to its exposure to proteases within endo-/lysosomes. Furthermore, the expression of a dominant-negative version of the GTPase, Rab4a, which inhibits recycling to the plasma membrane, increases the production of PrP^{Sc} in infected cells (Beranger et al., 2002). In addition, it has been proposed that PrP^{Sc} formation does not require cell-surface recycling and occurs in an intracellular compartment (Beranger et al., 2002). Taken together, it is likely that PrP^{Sc} may be generated either at the cell surface or at some point along the endocytic pathway before exposure of the substrate, PrP^{C}, to lysosomal proteases.

Baron et al. (2002) showed that insertion of PrP^{C} into membranes facilitates PrP conversion. There is also evidence that so-called "lipid rafts" may be the sites of conversion since PrP^{Sc} could be found, along with PrP^{C}, in "rafts" (Taraboulos et al., 1995; Vey et al., 1996; Naslavsky et al., 1997; Baron et al., 2002; Botto et al., 2004). In fact, when cells were depleted of cholesterol, PrP^{C} degradation was diminished and generation of PrP^{Sc} was reduced (Taraboulos et al., 1995). These reports would support that biogenesis of PrP^{Sc} is regulated by a cholesterol-dependent mechanism in rafts although depletion of sphingolipid, another raft component, unexpectedly showed the opposite effect, i.e., PrP^{Sc} formation was increased (Naslavsky et al., 1999). Engineered transmembrane forms of PrP^{C} that are not directed to rafts do not serve as substrates for PrP^{Sc} formation in PrP^{Sc}-infected cells (ScN2a) (Taraboulos et al., 1995; Kaneko et al., 1997), and pharmacological compounds disrupting rafts inhibit PrP^{Sc} formation (Taraboulos et al., 1990; Mange et al., 2000; Marella et al., 2002). Thus, rafts, microdomains formed in the membrane to produce an ordered lipid environment, have attracted attention as a candidate site for the generation of PrP^{Sc}.

So far, the vast majority of immunolocalisation experiments, with only a few exceptions (see, e.g., Taraboulos et al., 1990; Arnold et al., 1995; Vey et al., 1996; Fevrier et al., 2004), have been performed without PK digestion after permeabilisation – a treatment that would be appropriate to abolish PrP^{C} (Taraboulos et al., 1990; Prusiner, 2001), as was also reported for formic acid treatment (Kristiansen et al., 2007). Therefore, detection of PrP was not always selective for PrP^{Sc}, even if a denaturation step with 6 M guanidine hydrochloride or thiocyanate (GdnHCl, GdnSCN) was included, which allows staining of PrP^{Sc} without affecting PrP^{C} (Taraboulos et al., 1995).

In order to overcome problems of specificity apparent in previous reports, we first used conditions detecting either PrP^{Sc} or PrP^{C} in ScN2a cells. We were able to detect PrP^{Sc} at the plasma membrane and we obtained evidence for endocytosis of PrP^{Sc} via clathrin-coated pits and transport through early endosomes to late endosomes/lysosomes. Since PrP^{C} resided at the same sites, our findings are consistent with the $PrP^{C} \rightarrow PrP^{Sc}$ conversion occurring either at the plasma membrane or in endo-/lysosomal compartments. In ScN2a cells, lipid bodies (LBs), which are organelles harbouring PrP^{C} in Jurkat cells (Reuter et al., 2004), were not involved in transport and release of PrP^{Sc}. Instead, our analysis showed the release of PrP by exocytosis, i.e., via exosomes and by compact electron-dense masses. This represents a potential pathway for infection, in addition to release by decaying dead cells (Laszlo et al., 1992).

Materials and methods

Cell culture

N2a cells (American Type Culture Collection) were maintained in Dulbecco's modified Eagle's medium

(DMEM) (Invitrogen, Paisly, UK), and ScN2a cells (see below) in OptiMEM (Invitrogen), both supplemented with 10% foetal calf serum (FCS, Biochrom, Berlin, Germany), 100 units/ml penicillin, 100 µg/ml streptomycin (Invitrogen) and 2 mM glutamine (Invitrogen). The cells were cultivated at 37 °C and 5% CO_2.

Infection of N2a cells with scrapie

The highly susceptible clone H6 of N2a cells (Zhang et al., 2002) was infected with the 22L strain (kind gift of Prof. S. Lehmann, Montpellier, France) as described previously (Zhang et al., 2002), leading to persistent infection. Such cultures were termed "ScN2a". About 80% of the cells in ScN2a were positive for PrP^{Sc} as determined by immunofluorescence (IF).

Immunofluorescence

N2a or ScN2a cells were seeded to semi-confluence on glass coverslips. In some cases the cells were treated with 1 µg/ml ConA-A594 (Molecular Probes, Paisley, UK). ConA was dissolved in phosphate-buffered saline (PBS) supplemented with 1 mM $MgCl_2$ and 1 mM $MnCl_2$. Alternatively, 100 µM oleic acid (O-1008, Sigma) was added prior to fixation. The cells were fixed with 4% formaldehyde, freshly prepared from paraformaldehyde, and simultaneously permeabilised with 0.1% digitonin (D-141, Sigma) for 1 h at room temperature (RT). In case of ScN2a cells, a denaturation step with 6 M GdnHCl for 10 min followed. After blocking with 1% bovine serum albumin (BSA) for 30 min at RT, the cells were incubated with the primary antibody (AB) (6H4, 1:1000, kindly provided by Prionics, Zurich, Switzerland; Limp2, 1:50, sc-25867, Santa Cruz, Heidelberg, Germany; EEA1, 1:200, sc-6415, Santa Cruz; Stuermer et al., 2001; Reuter et al., 2004; Langhorst et al., 2008) in 1% BSA for 30 min at 37 °C and then, after appropriate washing, with the fluorescently labelled secondary AB (donkey anti-goat [DαG] Cy3, 705-166-147, Jackson ImmunoResearch, Suffolk, UK; goat anti-mouse [GαM] A488, Molecular Probes; GαM A546, Molecular Probes) diluted 1:1000 in 1% BSA for 30 min at 37 °C. Staining of lipid bodies was performed with 1 µg/ml Bodipy 499/508 (Molecular Probes) in PBS for 15 min at RT.

Assay for the detection of PrP^{Sc} at the plasma membrane

ScN2a or N2a cells (2×10^5) were grown on 24-well Lumox™ multiwell dishes pretreated with poly-L-lysine (0.2 mg/ml) for 1 h at RT. Twenty-four hours later the cells were fixed and permeabilised with 8% formaldehyde/0.1% glutaraldehyde and 0.1% digitonin for 1 h at RT. Cells were incubated with PK (20 µg/ml) for 15 min at 37 °C. Digestion was stopped with 2 mM phenylmethylsulphonylfluoride (PMSF, Sigma) for 15 min at RT. The cells were denatured with 6 M GdnHCl for 10 min. After blocking with 1% BSA for 30 min at RT, the cells were incubated with primary and secondary ABs diluted in 1% BSA for 30 min at 37 °C.

Image acquisition

Images were taken with laser scanning microscopy (LSM 510 Meta, Zeiss, Jena, Germany). Images were processed with Adobe Photoshop or Image J.

Electron microscopy (EM)

ScN2a cells (5×10^6) were seeded on 6-cm Lumox™ multiwell dishes (Greiner, Frickenhausen, Germany) pretreated with poly-L-lysine-hydrobromide (0.2 mg/ml, P-1399, Sigma) for 1 h at RT. Cells were first fixed and then subjected to the various processing steps, including permeabilisation, PK digestion, GdnSCN denaturation, dehydration and embedding. Other samples were treated in a similar way before fixation. In some cases incubation with ABs and gold conjugates was performed before embedding. Alternatively ABs and gold conjugates were applied only to ultrathin sections. In some experiments, pre- and post-embedding labelling was combined. Details are given in the figures.

Fixation and PrP^{Sc}-specific treatment was as follows. Cells were fixed and simultaneously permeabilised with 8% formaldehyde/0.1% glutaraldehyde first for 1 min, then in the same fixative supplemented with 0.1% digitonin, in 0.1 M piperazine-*N*,*N*'-bis(2-ethanesulfonic acid) (PIPES, Sigma) buffer pH 7.2, for 1 h at RT. Cells were washed three times for 10 min with PIPES. PK digestion (20 µg/ml, P-2308, Sigma) was performed for 15 min at 37 °C. The digestion was stopped with 2 mM PMSF in 0.1 M PIPES for 15 min at RT. The denaturation step was performed in an ascending and descending sequence in 1-molar steps from 1 to 6 M GdnSCN, each step with 5 min duration. This procedure provides better preservation of the ultrastructure of the cells than single-step denaturation with 6 M GdnSCN. (Note that, after washing with 0.1 M PIPES, some samples were incubated directly with the primary AB [6H4, Limp2, EEA] and the gold conjugate [pre-embedding labelling] after blocking free aldehyde groups as described below). For details, see text and figure legends. Samples were dehydrated with increasing ethanol series, before embedding in the methacrylate resin LR-Gold (London Resin, London, UK).

Section labelling was performed after masking free aldehyde groups with 50 mM glycine and BSA-C (BioTrend, Cologne, Germany) in PBS. For immuno-gold EM analysis, apart from materials

mentioned above, the following mono- and polyclonal ABs (mAB, pAB), respectively, and gold conjugates of 5 and 10 nm (Au_{5nm} and Au_{10nm}), respectively, were used: Protein A (pA)-Au_{5nm} and $pA_{10\ nm}$, goat anti-mouse (GαM) F(ab)$_2$-gold conjugates and GαM pABs. ABs and gold conjugate sources as well as embedding were as described previously and as specified in the respective figure legends. Analysis was performed with a Zeiss electron microscope type EM10.

Isolation of lipid bodies

ScN2a were seeded on 15-cm dishes. Six hours later cells were treated with 300 µM oleic acid overnight. The isolation was performed as previously described in detail (Weller et al., 1991; Reuter et al., 2004).

Western blots

ScN2a were lysed with 10 mM Tris-HCl, pH 7.5, 100 mM NaCl, 10 mM ethylenediamine tetra-acetic acid (EDTA, Sigma), 0.5% Triton-X-100, 0.5% deoxycholic acid sodium salt (DOC, Sigma), incubated with PK (50 µg/ml) for 30 min at 37 °C and precipitated with 4 volumes of ice-cold methanol. Samples were centrifuged for 30 min at 4000*g* at 4 °C. Pellets were treated with 6 M GdnHCl for 10 min and precipitated once again overnight with 4 volumes of methanol. After centrifugation at 4000*g* for 30 min at 4 °C the pellets were air dried and dissolved in TNE buffer (150 mM NaCl, 50 mM Tris-HCl, pH 7.5, 5 mM EDTA). Protein samples were separated by reducing SDS-PAGE followed by blotting on PVDF membranes (GE Healthcare, Freiburg, Germany) and blocked with 5% milk in Tris-buffered saline supplemented with 0.05% Tween 20 (TBST). The blot was incubated with primary and secondary ABs in 5% milk/TBST for 1 h each at RT. The secondary ABs were coupled with horseradish peroxidase (DAKO Cytomation, Glostrup, Denmark). Detection was performed with ECL Advance Western Blotting Detection Kit (GE Healthcare, Munich, Germany) using an LAS 1000 camera (Fujifilm, Düsseldorf, Germany).

Results

IF detection of PrP^{Sc} in ScN2a cells after denaturation with 6 M GdnHCl

In order to allow efficient staining of PrP^{Sc} in scrapie-infected N2a cells (ScN2a) using available ABs for light and electron microscopy, PrP^{Sc} has to be denatured with 6 M GdnHCl (Taraboulos et al., 1990). One aim of our study was to compare the localisation of PrP^{C} and PrP^{Sc}. First, non-infected N2a cells were stained for PrP^{C} with or without the denaturation step. In non-infected cells, PrP^{C} was localised to the plasma membrane (Fig. 1A and B), as expected. In some cells a weak intracellular PrP^{C} signal was found. Next, ScN2a cells were stained with AB 6H4 with or without prior denaturation of the samples with 6 M GdnHCl (Fig. 1C and D). Without GdnHCl, only PrP^{C} was stained at the cell surface. In the presence of GdnHCl there were additional strong signals within the cell which were apparently caused by PrP^{Sc} because they were not found in ScN2a without GdnHCl treatment or in non-infected N2a cells (Fig. 1A–C). In fact, the denaturation step with 6 M GdnHCl is an appropriate and well-established method to detect PrP^{Sc} (Taraboulos et al., 1990). Although in Fig. 1 no PK digestion had been performed, the simultaneous detection of PrP^{C} was apparently minimised since the detector gain in confocal microscopy had to be increased considerably in order to record any signal at all (Fig. 1C, no GdnHCl treatment). Nevertheless, the 6H4 signal at the plasma membrane could be caused both by PrP^{Sc} and PrP^{C}. The detection upon treatment with 6 M GdnHCl was also performed with other ABs directed against PrP, i.e. 12F10 (mouse mAB) (Krasemann et al., 1996) and Kan72 (rabbit polyclonal serum obtained by immunisation with peptide 89–112 of the prion protein) (Hölscher et al., 1998), resulting in the same staining pattern.

For the localisation of PrP^{Sc}, particularly at the plasma membrane, an additional PK treatment was necessary to destroy any residual PrP^{C} present at the plasma membrane (Fig. 2). For the localisation of PrP^{Sc} in intracellular compartments by IF (see below, Figs. 3, 4 and 10A) PK digestion was omitted. Incubation with PK under conditions of sample preparation required for IF analysis turned out to severely affect the possibility of staining of organelles (data not shown). Fortunately, PK digestion was not necessary in this case, because ScN2a cells could be easily distinguished from uninfected N2a cells by the criterion of intracellular PrP^{Sc} accumulation, in contrast to uninfected N2a cells, which exhibited PrP staining at the cell surface only. The denaturation step did not affect staining of PrP^{C}, whereas it was necessary for the detection of PrP^{Sc} (Fig. 1). Thus, in our IF-colocalisation experiments of PrP^{Sc} with EEA1, Limp2 and LBs solely intracellular signals from PrP^{Sc} were examined (Figs. 3, 4 and 10A). In this case, the presence of PrP^{C} was excluded. The simultaneous detection of PrP^{C} and PrP^{Sc} was also prevented by the choice of the appropriate detector gain (see above).

IF localisation of PrP^{Sc} in ScN2a cells at the plasma membrane

In previous reports the detection of PrP^{Sc} at the cell membrane was mostly investigated by the isolation of

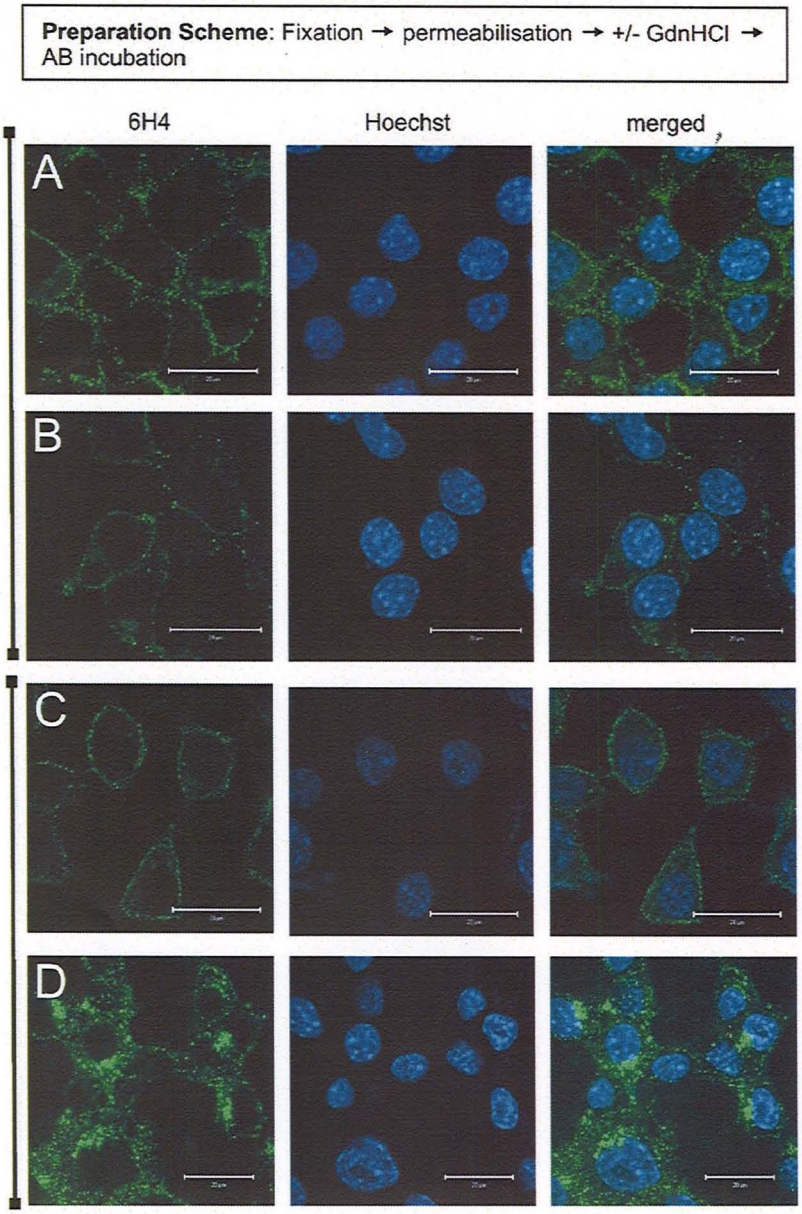

Fig. 1. Detection of PrP^{Sc} in ScN2a cells by IF after denaturation with 6 M GdnHCl (no PK digestion). Uninfected N2a cells (A, B) and scrapie-infected ScN2a cells (C, D) were seeded on coverslips to 50% confluence. Cells were fixed, permeabilised, denatured with 6 M GdnHCl (B, D) or not treated with GdnHCl (A, C). Cells were stained with 6H4 and GαM A488 for PrP. Nuclei were counterstained with Hoechst 33342. Note that only in ScN2a cells PrP^{Sc} could be visualised, since this occurred only after denaturation with 6 M GdnHCl. Also note that in (C), detector gain had to be increased considerably to record any signal at all. Bars: 20 μm.

detergent-resistant membranes (Vey et al., 1996; Naslavsky et al., 1997). Here we show by IF that PrP^{Sc} was located at the cell membrane (Fig. 2). To ascertain that those signals were due to PrP^{Sc}, rather than PrP^{C}, ScN2a cells were treated with PK, followed by denaturation with GdnHCl before AB incubation. It should be noted that permeabilisation of the cells could not be avoided because GdnHCl treatment per se is sufficient to permeabilise cells.

Although PK digestion is a harsh procedure, the majority of the cells remained intact. In a first step we tested whether the PrP^{C} signal vanished after PK treatment. As shown in Fig. 2B the typical PrP^{C} signal at the plasma membrane of N2a cells disappeared when

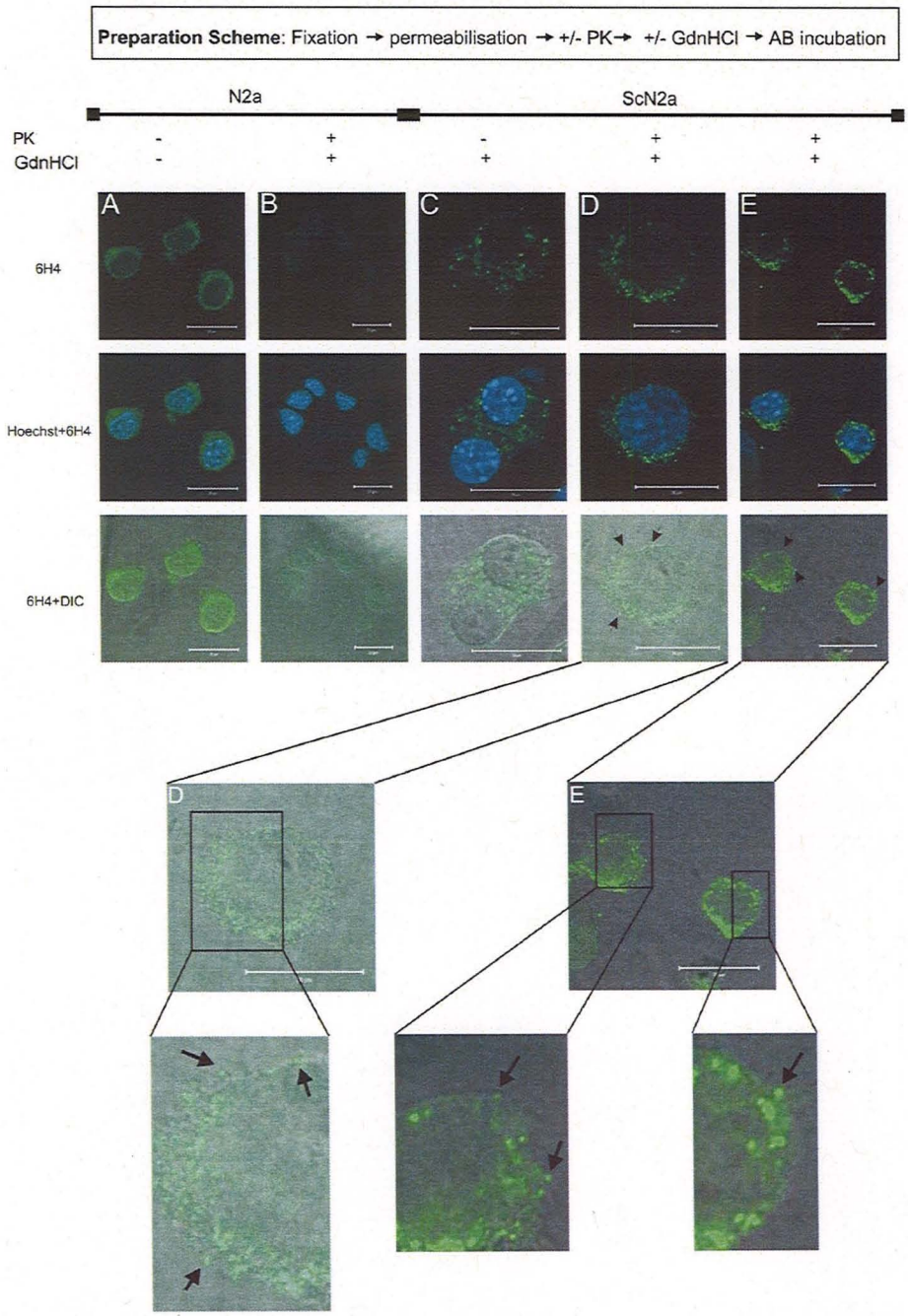

Fig. 2. IF localisation of PrP^{Sc} in ScN2a cells at the plasma membrane. N2a (A, B) or ScN2a (C–E) cells were cultured on poly-L-lysine-coated Lumox dishes. After fixation, permeabilisation, PK digestion and GdnHCl incubation the cells were stained with 6H4 and GαM A488 for PrP. The nuclei were counterstained with Hoechst 33342. Upon treatment with PK, the PrP^{C} signals were lost (B) and only the signal for PrP^{Sc} remained intact in ScN2a cells (D, E). Arrowheads indicate the presence of PrP^{Sc} at the plasma membrane. Bars: 20 μm.

the cells had been treated with PK. As a next step, the procedure was extended to ScN2a cells. Upon PK treatment abundant PrP^{Sc} signals could be found mainly intracellularly in almost all cells, but to a much lesser extent also at the plasma membrane (Fig. 2D and E). A higher magnification of Fig. 2D and E (arrowheads) revealed the appearance of PrP^{Sc} precisely at the plasma membrane.

Treatment of ScN2a cells with ConA

Since PrP^{Sc} is glycosylated like PrP^{C}, containing mannose and glucose (Endo et al., 1989; Rudd et al., 1999), and since PrP^{Sc} is present at the plasma membrane (Fig. 2), we had anticipated that PrP^{Sc} could possibly be endocytosed together with the lectin concanavalin A (ConA). ConA can be expected to bind to the glucosyl and mannosyl residues of glycosylated PrP (Bernhard and Avrameas, 1971). If this were to occur at the cell surface, it should drive internalisation of PrP, as has been established with some other cell-surface glycoproteins (Maher and Molday, 1981). This could yield valuable information on the trafficking process of PrP.

Already after 10 min, ScN2a cells displayed ConA staining of the cell membrane, whereas after 30 min the stained material appeared within the cell and was mostly intracellular after 100 min. Thus, ConA binds to cell membrane-bound glycoproteins as expected (Fig. 3). However, as PrP^{Sc} is already present within the cell without ConA treatment, it is hard to decide whether ConA could accelerate the internalisation of the small portion of PrP^{Sc} normally present at the plasma membrane. Parallel experiments with ConA-treated uninfected N2a cells indicated that ConA was internalised but the amount of PrP^{C} at the plasma membrane stayed the same and no internalisation of PrP^{C} could be observed (data not shown), thus indicating that ConA did not function as an appropriate compound to drive

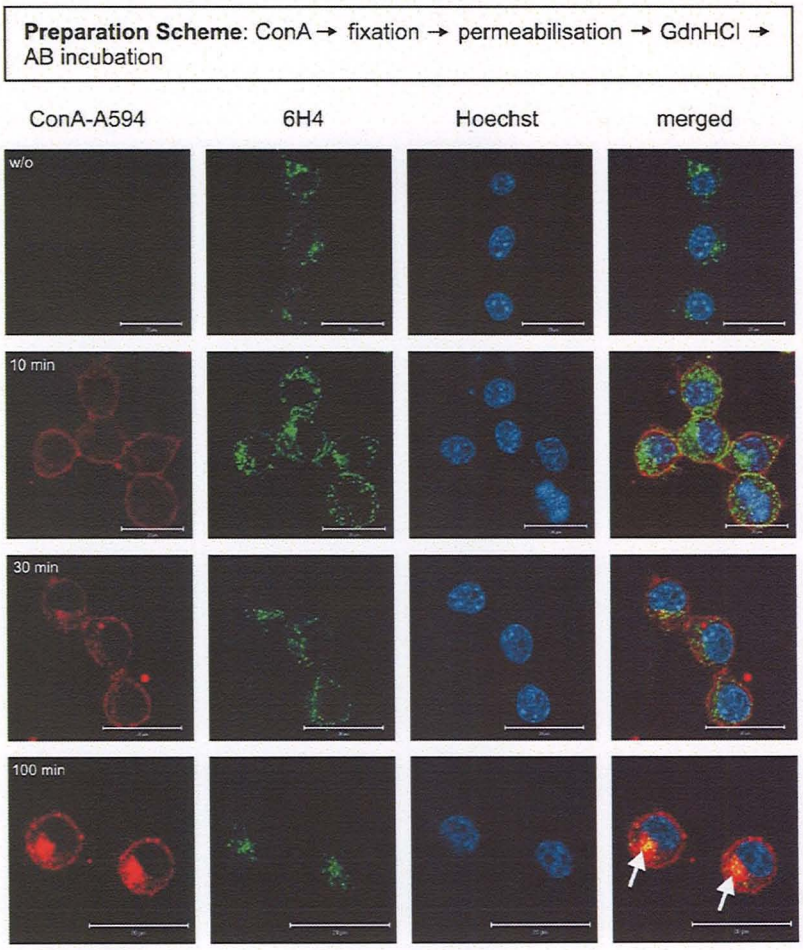

Fig. 3. Endocytosis in infected ScN2a cells analysed with ConA (no PK treatment). ConA-A594 (1 µg/ml) was added to scrapie-infected ScN2a cells for 10, 30 or 100 min. After fixation, permeabilisation and denaturation with 6 M GdnHCl the cells were stained for PrP^{C} with AB 6H4 and GαM A488. Nuclei were counterstained with Hoechst 33342. The merged pictures were analysed for colocalisation of ConA and PrP. Note that under these conditions intracellular signals represent PrP^{Sc} as they depend on GdnHCl denaturation (see Fig. 1). At 100 min a partial colocalisation of ConA-A594 and PrP^{Sc} was observed (arrows), which, however, may not necessarily be due to internalisation of PrP^{Sc} from the plasma membrane because the major part of PrP^{Sc} had already been within the cell prior to incubation with ConA-A594. ConA ingestion was not paralleled by increased PrP uptake. Bars: 20 µm.

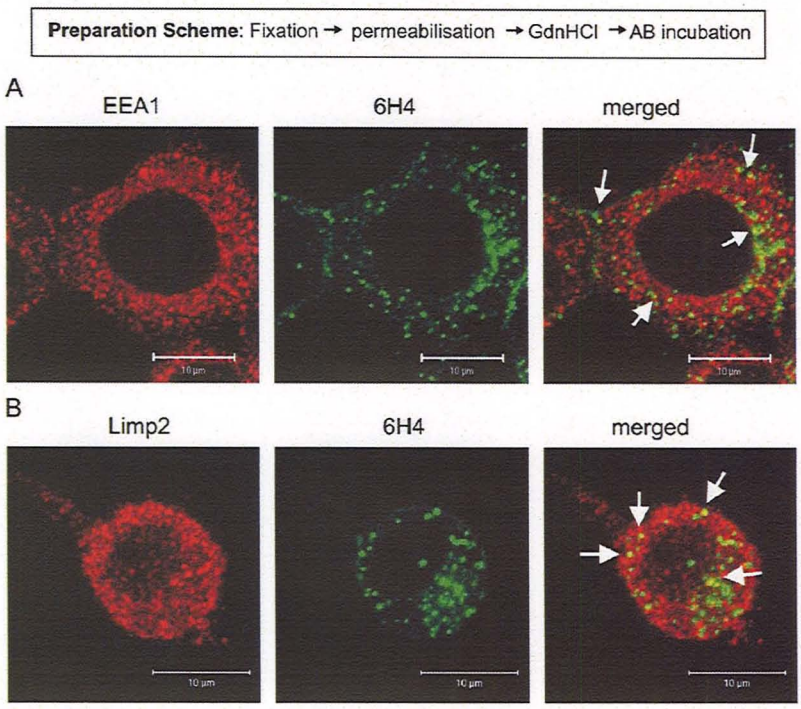

Fig. 4. Colocalisation of PrP^{Sc} with endosomal and lysosomal markers (no PK treatment). Cells were fixed, permeabilised, denatured with 6 M GdnHCl and incubated with the 6H4 AB and GαM A488 for PrP, with EEA1 and DαG Cy3 for early endosome labelling (A) or Limp2 and DαG Cy3 for late endosome/lysosome labelling (B). Representative colocalisations are indicated by arrows. Note that colocalisation is rare. Bars: 10 µm.

internalisation of PrP. Application of ConA proved useful, nevertheless, for the following reason: Since after 100 min ConA treatment a partial colocalisation of ConA with PrP^{Sc} could be seen inside ScN2a cells (Fig. 3, arrows), this experiments shows that PrP^{Sc} ends up in the same compartment as ConA, albeit in much smaller amounts. Since ConA is known to accumulate in lysosomes (Hansen et al., 1993; Yi and Tang, 1999) PrP^{Sc} was probably targeted to the same organelle, as is the case for the bulk of surface glycoproteins.

IF colocalisation of PrP^{Sc} with endosomal and lysosomal markers

Since ConA was not able to trigger internalisation of PrP, we decided to focus on colocalisation aspects. After fixation, permeabilisation and denaturation with 6 M GdnHCl cells were stained with 6H4 AB, together with the early endosome and late endosomes/lysosome markers, EEA1 and Limp2, respectively. Confocal images were analysed for colocalisation with PrP^{Sc} by applying the criterion of intracellular GdnHCl-dependent PrP signals (see Fig. 1). In almost every focal plane of a z-stack, several colocalisations were found (Fig. 4), but the major part of PrP^{Sc} accumulated outside early endosomes and late endosomes/lysosomes. Although these ScN2a cells were not treated with PK, it is unlikely that PrP^{C} contributed substantially to the PrP staining for the following reasons: First, the PrP^{C} signal was considerably weaker than the PrP^{Sc} signal. (Note that in Fig. 4 the detector gain was set in such a way as to dim the PrP^{C} signal almost completely.) Second, colocalisation only occurred at intracellular sites, where PrP^{C} signals are known to be very weak (Fig. 1).

Immuno-gold EM analyses of PrP^{C} in ScN2a cells at the cell surface and in intracellular compartments after treatment with PK and GdnSCN

In order to investigate the localisation of PrP more precisely, EM analyses were performed. In a first step, the normal cellular PrP^{C} was to be detected in ScN2a cells (Figs. 5–7). For this purpose, ScN2a cells were incubated at 4 °C with mAB 6H4, followed by labelling with $F(ab)_2$-Au_{10nm} in vivo, mild aldehyde fixation, permeabilisation, PK digestion and GdnSCN denaturation. It should be emphasised that PK digestion and GdnSCN denaturation were applied only after AB

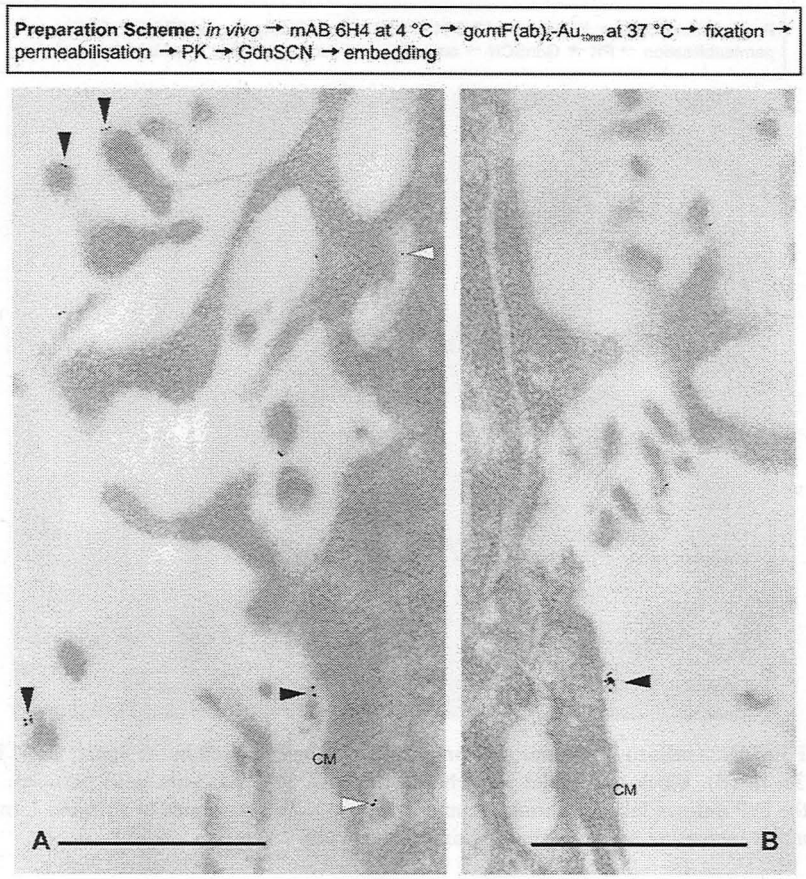

Fig. 5. Immuno-gold labelling of PrP^C in ScN2a cells. Cells reveal individual gold grains and occasional gold clusters on the cell membrane (black arrowheads), i.e., on filopodia (A) and on smooth areas (B), respectively. Some label is also detected in invaginations or vacuoles (white arrowheads). Due to the preparation scheme, the antigen labelled should be mainly PrP^C. Note the small size of microdomains with only up to five Au_{10nm} labels (A) or occasional larger sites of ~50 nm (B). CM, cell membrane. Bars: 1 μm.

incubation, so that the majority of label will be on PrP^c. After PK digestion also the ABs are digested, but the inert gold granules remain unaffected and stayed at the sites where PrP had been present. Filopodia showed clearly individual gold granules and speckles of up to five granules (Fig. 5A) as well as a larger gold cluster of ~50 nm on a smooth part of the cell membrane (Fig. 5B).

This specification of the labelling might also hold true for data presented in Fig. 6, which showed under the same conditions that 6H4 labelling occurred in lysosomes identified by anti-Limp2 AB post-embedding labelling. Both types of labelling were associated both with membranes and electron-dense materials, the polymorphous appearance of which was typical of lysosomes.

Other investigators detected PrP in exosomes in GT1-7 cells, rabbit epithelial Rov cells and Mov cells (Fevrier et al., 2004; Vella et al., 2007), but we additionally detected the release of PrP by exosomes in ScN2a cells engaged in contact with other cells. Furthermore, PrP-positive electron-dense material of irregular shape was observed, which was probably exocytosed (Fig. 7). In this experiment ScN2a cells were treated as described above. We detected release of 6H4 mAB/GαM $F(ab)_2$-Au_{10nm}-labelled materials of two kinds from ScN2a cells (Fig. 7). First, we saw release of labelled vesicles from larger vesicles by exocytosis, which clearly are exosomes originating from multivesicular bodies (Fig. 7, bottom) as they were also found inside the cytoplasm (not shown). Moreover, under these conditions, label has been detected in association with opaque electron-dense material of irregular shape (Fig. 7, top). Here, the actual occurrence of exocytosis was less clear. But even if the picture were to show endocytosis, this material must have been released previously from the ScN2a cells. Due to pre-embedding labelling, only the circumference of such amorphous clumps is labelled. This material is clearly different from LBs analysed separately (see below).

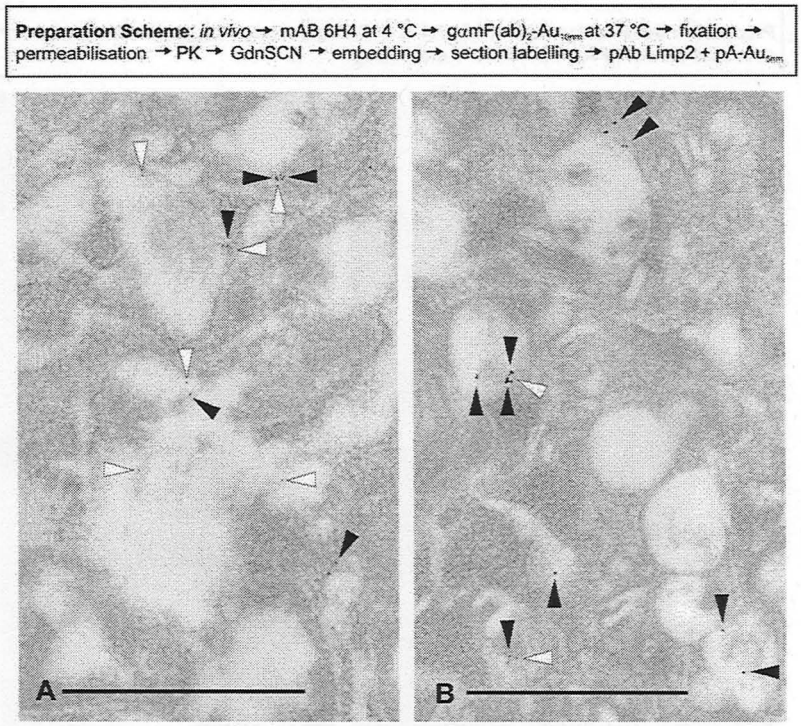

Fig. 6. Transport of PrP in ScN2a cells to lysosomes. The preparation scheme is given in the figure. GαM $F(ab)_2$-Au_{10nm} incubation lasted 1 h in (A) and 3 h in (B). Black and white arrowheads point to 10- and 5-nm gold particles, respectively. Due to the preparation sequence, the PrP antigen labelled should be mainly PrP^C. Note occurrence of PrP and Limp-2 in the polymorphous lysosomes, with PrP content increasing with crosslinking time. Bars: 1 μm.

Immuno-gold EM analysis of PrP^{Sc} in ScN2a cells in intracellular compartments after treatment with PK and GdnSCN

Stringent selectivity of PrP^{Sc} localisation in intracellular compartments was obtained at the EM level by AB labelling after PK. In addition, gentle denaturation with an ascending and descending series of solutions of 1 to 6 M GdnSCN in 1 M increment was carried out to improve ultrastructural preservation. Nevertheless, the morphology of the cells did change and the frequency and density of labelling was much lower than we had previously observed with uninfected, untreated cells (Langhorst et al., 2008).

After mild aldehyde fixation ScN2a cells were permeabilised and treated with PK and GdnSCN, followed by incubation with 6H4 AB and its visualisation by Au_{5nm}. This pre-embedding labelling was appropriate to pinpoint antigens within organelles. These were identified in the current experiments by post-embedding labelling with anti-EEA1 ABs and Au_{10nm} labelling (Fig. 8B–D). The 6H4 labelling was enhanced by exposure of ultrathin sections to 6H4 ABs and Au_{5nm} conjugates – a method we had previously applied successfully for signal enhancement (Lang et al., 1998).

Not only could we detect PrP^{Sc} labelling in compartments positive for anti-EEA1 ABs, i.e., early endosomes, of rather polymorphic appearance and frequently with irregular processes or protrusions (Fig. 8B–D), but we also saw uptake of PrP^{Sc} via bristle-coated (clathrin-type) endocytotic vesicles characterised by their spiny coats (Fig. 8A). In another set of experiments, ScN2a cells were subjected to mild aldehyde fixation, permeabilisation, PK digestion and GdnSCN denaturation before embedding and section labelling by two ABs, first by 6H4 AB/Au_{10nm} and second by anti-Limp2/Au_{5nm} (Fig. 9). Gold grains were associated with lysosomes, i.e., their wrapping membrane and occasionally with irregular contours inside the organelle. Thus, based on ultrastructure and Limp2 content they can be identified as late endosomes/lysosomes containing PrP^{Sc} (Langhorst et al., 2008).

PrP^{Sc} and lipid bodies

In Jurkat T cells PrP^C has been found to be localised to lipid bodies (LBs) that were observed to be exocytosed (Reuter et al., 2004). Although LBs are mainly organelles for lipid storage, they can also participate in signalling and membrane trafficking

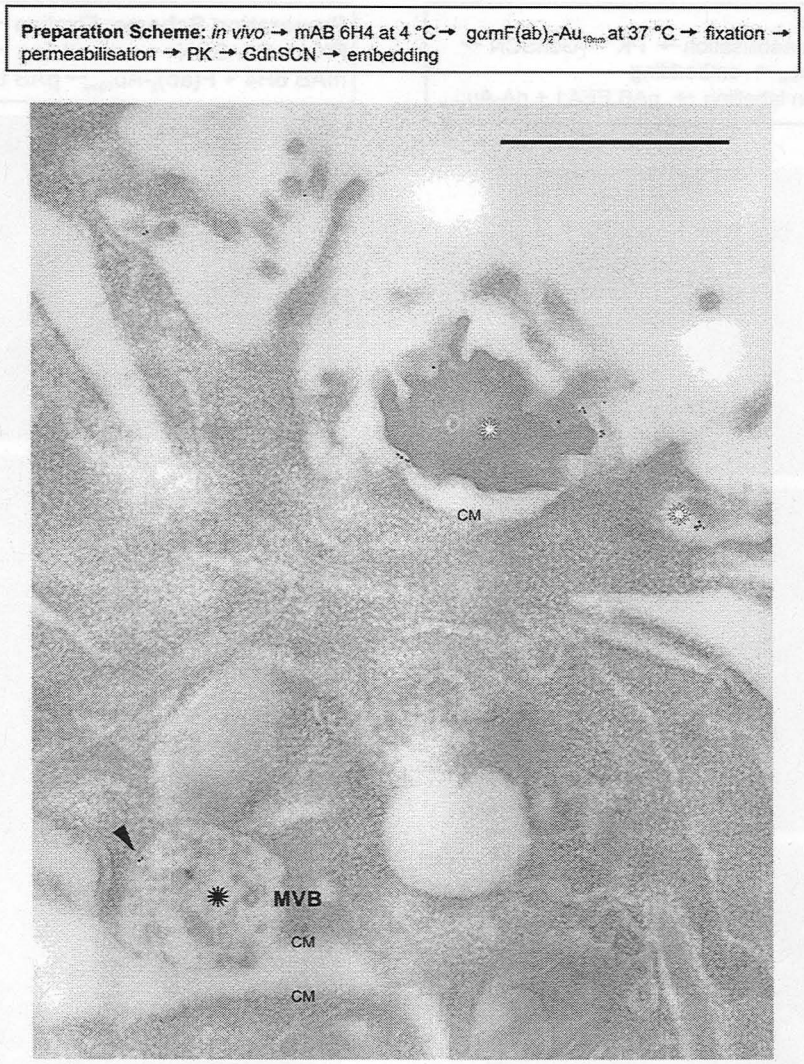

Fig. 7. Release of PrP from ScN2a cells. PrP is bound to homogeneous material (white asterisks, with gold label attached) or associated with exosomes (multivesicular body [MVB], labelled with black asterisk and black arrowhead at gold labelling sites) released by exocytosis. Due to the preparation scheme, the antigen labelled should be mainly PrP^C. CM, cell membranes of two adjacent cells. Bar: 1 µm.

(Liu et al., 2004). Therefore, the question arose if lipid droplets might play a role in the transport and release of PrP^{Sc}. Following previously published protocols (Reuter et al., 2004) we investigated whether PrP^{Sc} could actually reside in LBs. To enhance the generation of LBs, ScN2a were treated with 100 µM oleic acid overnight. After fixation, permeabilisation and denaturation the cells were stained with 6H4 AB for PrP^{Sc} and with Bodipy 493/503 for LBs (Fig. 10A). No colocalisation of PrP^{Sc} and LBs could be detected. In addition, we isolated LBs from ScN2a cells by sucrose gradient centrifugation where LBs float on the sucrose cushion. Fractions were collected from the gradient, digested with PK, denatured and methanol precipitated. Western blot analysis demonstrated that PrP^{Sc} was present only in fractions 3 (scarce) and 4 (abundant) (Fig. 10B). To make sure that fraction 1 indeed contained LBs, an aliquot of this fraction was stained for LBs with Bodipy 493/503 (Fig. 10C). In fraction 1, which contained the LBs, PrP^{Sc} was not detectable (Fig. 10B). In contrast, LBs isolated from uninfected N2a cells contained PrP^C (data not shown).

Discussion

The aim of this study was to unravel by light and electron microscopic immuno-labelling the subcellular localisation of PrP^{Sc} – a rather challenging task in view

Preparation Scheme:
A-D: Fixation → Permeabilisation → PK → GdnSCN → mAB 6H4 + $F(ab)_2$-Au_{5nm} → embedding
in case of B-D: section labelling → pAB EEA1 + pA-Au_{10nm}

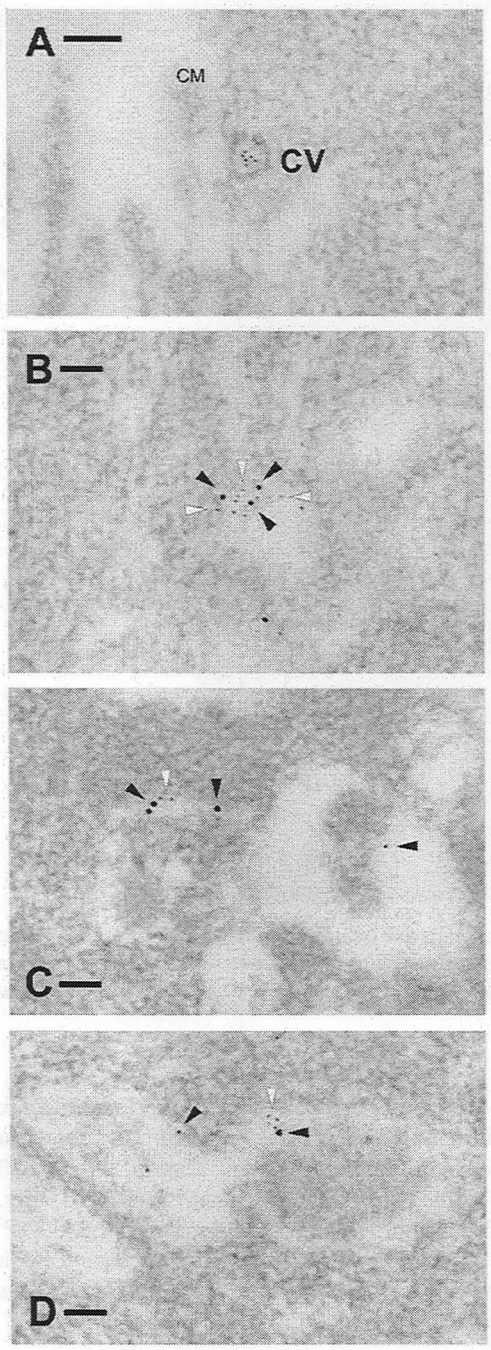

Fig. 8. Internalisation of PrP^{Sc}: uptake via coated vesicles (A) and examples of delivery to early endosomes (B–D). The preparation scheme is given in the figure. During section labelling with anti-EEA1 pAB→pA-Au_{10nm}, labelling for PrP was enhanced by an additional incubation with 6H4mAB and GαM pAB_{5nm}. CM, cell membrane; CV, coated vesicle. Bars: 0.1 μm.

Preparation Scheme: Fixation → permeabilisation → PK → GdnSCN → embedding → section labelling → mAB 6H4 + $F(ab)_2$-Au_{10nm} → pAB Limp2 + pA-Au_{5nm}

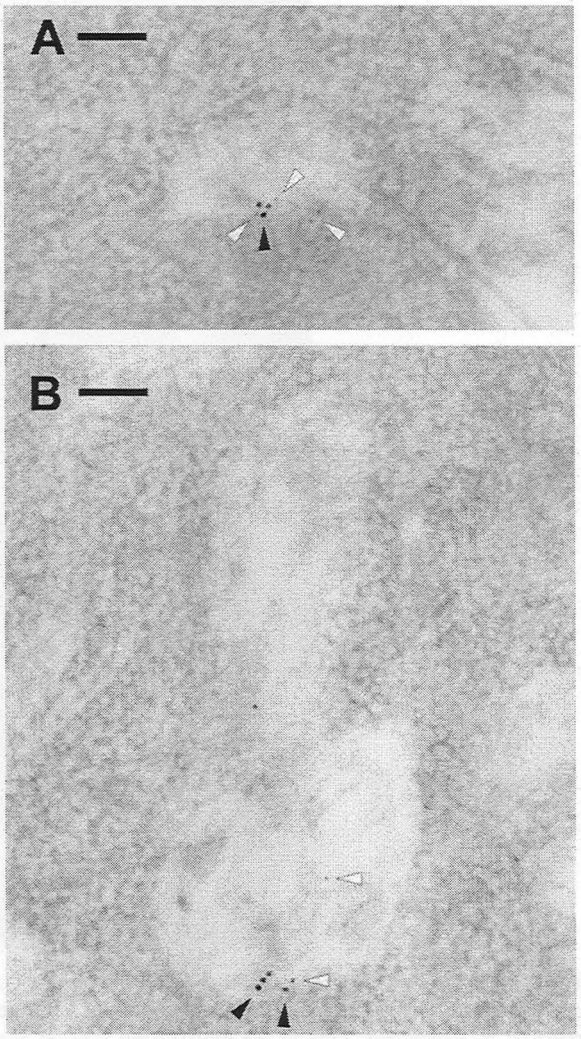

Fig. 9. Examples of PrP^{Sc} delivery to lysosomes. The preparation scheme is given in the figure. Black and white arrowheads indicate PrP and Limp2 localisation, respectively. Bars: 0.1 μm.

of the necessity to apply several harsh treatments during sample preparation and the restricted specificity of ABs available (see below). Whenever possible a clear distinction between PrP^{C} and PrP^{Sc} was made by the use of protease digestion and GdnHCl/GdnSCN denaturation. We now can show that PK-resistant PrP is located at the plasma membrane, in early endosomes and in late endosomes/lysosomes, but not in lipid bodies. Endocytosis of PrP^{Sc} apparently occurs via clathrin-coated pits. Exocytosis of PrP^{C} in ScN2a cells apparently takes place via exosomes and clumps of opaque materials (probably protein aggregates).

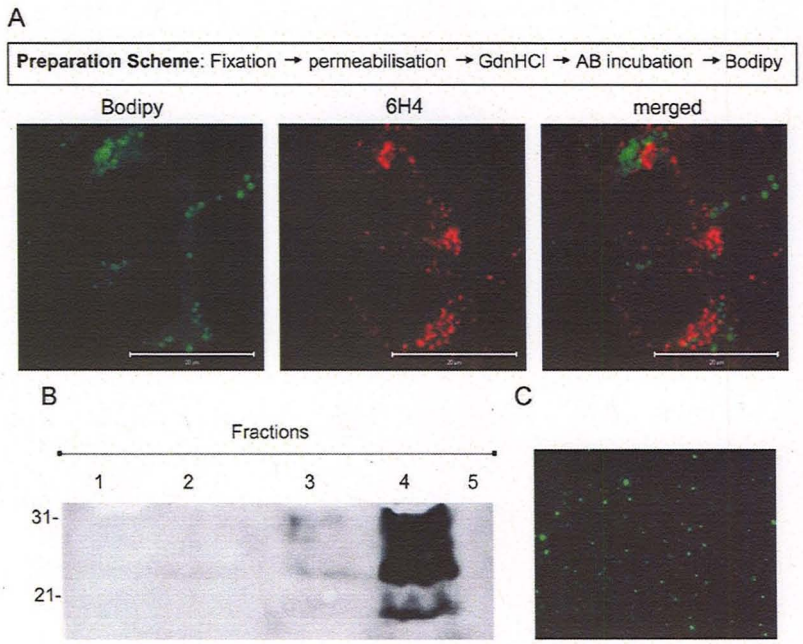

Fig. 10. PrP^{Sc} is not enriched in lipid bodies in ScN2a cells. ScN2a cells were incubated with 100 µM oleic acid overnight to enhance the production of LBs. (A) Cells were fixed, permeabilised and denatured with 6 M GdnHCl. No PK digestion was performed. Staining of LBs was performed with Bodipy 499/508. PrP was stained with AB 6H4 and GαM A546. No colocalisation could be detected. Bars: 20 µm. (B) Cells were fractionated by ultracentrifugation. The fractions were digested with PK, denatured with 6 M GdnHCl, precipitated with methanol, and subjected to SDS-PAGE and immunoblotting. For details, see Materials and methods. Only fractions 3 and 4 contained PrP^{Sc}, while the LB-containing fraction 1 did not show a PrP^{Sc} signal. (C) An aliquot of fraction 1 was stained with Bodipy 499/508 to confirm the presence of LBs in this fraction. Same magnification as in (A).

Technical issues relating to the detection of PrP^{Sc} in cultured cells

For several reasons it is rather difficult to unequivocally and selectively localise PrP^{Sc} by immunohistochemistry or immunocytochemistry. As no PrP^{Sc}-specific ABs suitable for microscopy exist, this problem had to be overcome by denaturation of PrP^{Sc} with 6 M guanidine (Taraboulos et al., 1990) which exposes the relevant epitopes to PrP-specific ABs. (N.B. 98% formic acid was also reported as an alternative to abolish PrP^{C} staining; Kristiansen et al., 2005). In our EM analyses we preferred to apply, after PK digestion, GdnSCN in graded concentrations in order to minimise structural damage that would invalidate ultrastructural analyses. This denaturation step causes a conformational change in PrP^{Sc}, such that in permeabilised cells the AB gains access to the antigen whose epitope is buried within the molecule or aggregates of molecules before denaturation (Caughey et al., 1991). Fig. 1D clearly shows the ability of AB 6H4 to stain PrP^{Sc} after denaturation with GdnHCl. Most of the PrP^{Sc} accumulated within the cell as demonstrated also in the literature (Caughey et al., 1991; Pimpinelli et al., 2005; Kristiansen et al., 2007). But the endogenous PrP^{C} was not destroyed and thus also detected at the plasma membrane in these experiments. In fact, the denaturation step did not prevent staining of PrP^{C} (Fig. 1B) in accordance with the literature (Taraboulos et al., 1990). However, since the distribution pattern of PrP^{C} and PrP^{Sc} differed from each other, we conclude that the intracellular staining is caused by PrP^{Sc}.

Additional specificity is provided by PK digestion of PrP^{C}, leaving the carboxy-terminal part of PrP^{Sc} unaffected, which was performed in some of our EM (Figs. 8 and 9) and particularly in IF experiments dedicated to the localisation of PrP^{Sc} at the plasma membrane (Fig. 2).

PK digestion turned out not to be feasible in IF experiments aiming at organelle labelling by ABs, due to the preparation conditions required for IF analysis. Even when PK digestion was omitted, in the experiments with ABs recognising EEA1, Limp2 and LBs (Fig. 4 and 10A), only intracellular signals from PrP^{Sc} were recorded since intracellular staining was abundant only in ScN2a cells, but scarce in non-infected cells (Fig. 1). Another approach to selectively visualise PrP^{Sc} after denaturation was to reduce detector gain in confocal microscopy to a level where the PrP^{C} signal in ScN2a cells vanished almost completely (Figs. 3, 4 and 8A).

More stringent selectivity of PrP^{Sc} localisation in early and late endosomes/lysosomes was obtained at the EM level after PK treatment, eventually combined with gold labelling of ultrathin sections. This may result from sufficient sensitivity provided by the fact that methacrylate sections are not smooth and may thus uncover some antigenic sites not accessible in whole mounts (Armbruster et al., 1982). But under the harsh methodological conditions (PK and GdnHCl) the antibodies would not achieve an abundant labelling that would be expected in cells not undergoing enzymatic and chemical treatment. Therefore, no quantitative analysis of immuno-gold labelling was performed. The amount of extra work required for quantification would be out of all proportion to the possible gain of information.

Localisation of PrP^{Sc} at the plasma membrane

In Fig. 2 we showed with a quite demanding experimental set-up the localisation of a small part of PrP^{Sc} at the plasma membrane. A PK step is crucial to destroy the endogenous PrP^{C} signal, but at the same time causes cells to detach from the substrate and does harm to cell structure. Besides growing cells on poly-L-lysine-coated Lumox dishes, a sufficient degree of aldehyde fixation and a mild permeabilisation seemed to be crucial for adherence of ScN2a cells. Surprisingly, the morphology of the PK digested cells was sufficiently intact and cell detachment was minimal. Staining of PrP^{Sc} was also possible (Fig. 2D and E). In conclusion, we have established the tools that allow selective localisation of PrP^{Sc} in cell cultures. We could clearly demonstrate, after digestion of PrP^{C} with PK, the presence of PrP^{Sc} at the plasma membrane. The conversion process has previously been proposed to take place at the plasma membrane (Vey et al., 1996; Naslavsky et al., 1997; Baron et al., 2002; Baron and Caughey, 2003; Botto et al., 2004), which is compatible with our results. We detected only small amounts of PrP^{Sc}, in contrast to other investigators (Borchelt et al., 1990; McKinley et al., 1991; Kristiansen et al., 2007), either because they used different scrapie strains or did not perform PK digestion or the relevance of cell density may not have been considered. Nevertheless, our result go well beyond those of other groups because we were able to visualise, by IF analysis, selectively PrP^{Sc} at the plasma membrane, the selectivity being due to PK digestion.

Stimulation of PrP endocytosis by ConA

In several sets of experiments we have attempted to stimulate the endocytosis of membrane-bound PrP^{Sc}. However, ConA does not seem to enhance the internalisation of PrP, although several publications have shown that the glycosyl residues relevant for binding do exist also in the PrP^{Sc} molecule (Endo et al., 1989; Rudd et al., 1999). Alternatively, ConA may be endocytosed with different kinetics than PrP^{Sc} molecules and ConA may not drive endocytosis of PrP^{Sc} in ScN2a cells. This is consistent with a report that analysed ConA-labelled cell-surface proteins in neuroblastoma cells (Maher and Molday, 1981). Although ConA labelled 20 different polypeptides, only four were internalised. Furthermore, as most of the PrP^{Sc} was already located within the cell before ConA treatment, the small portion of PrP^{Sc} available at the plasma membrane would not preponderate even when internalised. A more unlikely explanation of the different internalisation of ConA and PrP, respectively, may be the following: ConA and PrP are endocytosed via distinct internalisation pathways, i.e., not only via clathrin-coated, but also via non-clathrin-coated vesicles (Renau-Piqueras et al., 1985) and both mechanisms would agree with the pathway of uptake of GPI-anchored proteins from reggie/flotillin-based microdomains (Frick et al., 2007) including PrP^{C} (Langhorst et al., 2008). As far as PrP^{Sc} is concerned, we have seen up to now only the first pathway (this study).

Interestingly, after 100 min of ConA treatment PrP^{Sc} was found in the same organelles as ConA (Fig. 3), i.e., lysosomes (Herman and Albertini, 1982; Hansen et al., 1993; Yi and Tang, 1999). We decided not to perform other experiments of stimulation of endocytosis/kinetic studies, e.g., cell-surface biotinylation or other kinds of pulse-chase labelling (Pauly and Harris, 1998; Nunziante et al., 2003; Stuermer et al., 2004; Pimpinelli et al., 2005; Taylor et al., 2005) as they did not appear appropriate or promising. In particular, following crosslinking with ABs, PrP^{C} was shown to be endocytosed and to allow immunocytochemistry (Stuermer et al., 2004; Pimpinelli et al., 2005), but this method would not be appropriate for PrP^{Sc} endocytosis, since ABs could only bind to PrP^{Sc} after denaturation. Furthermore, administration of Cu^{2+} ions promoted endocytosis of PrP^{C} (Pauly and Harris, 1998; Nunziante et al., 2003; Taylor et al., 2005), but this was never shown for PrP^{Sc}. Finally, cell-surface biotinylation always included immunoprecipitation followed by Western blot analysis (Pauly and Harris, 1998; Nunziante et al., 2003; Taylor et al., 2005) but it is not appropriate for an in situ readout for the following reason: Although PrP^{Sc} can be a substrate for biotinylation (Vey et al., 1996), all of the cell-surface proteins would be labelled and therefore detection of the selective endocytosis process of PrP^{Sc} would be obscured by a massive background due to the labelling of the vast majority of cell-surface proteins with biotin.

Localisation of PrP^{Sc} in ScN2a cells

Several groups have demonstrated PrP^{C} in endosomal compartments (Shyng et al., 1993; Laine et al., 2001; Magalhaes et al., 2002; Prado et al., 2004; Langhorst et al., 2008). Others detected PrP^{C} in lysosomes upon crosslinking of PrP^{C} (Stuermer et al., 2004). Finally, it was reported that PrP^{C} is fully degraded in lysosomes (Caughey et al., 1991), and fast lysosomal degradation may explain the difficulty to detect PrP^{C} in these organelles.

In early publications it was postulated that the conversion process from PrP^{C} into PrP^{Sc} should take place in acidic compartments, such as the endo-/lysosomal system, or at the plasma membrane (Caughey and Raymond, 1991; Caughey et al., 1991; Borchelt et al., 1992; Taraboulos et al., 1992). Recently, evidence was provided by Paquet et al. (2007) showing that conversion most likely occurs in early endocytic compartments. Using both light and electron microscopy we detected PrP^{Sc} at all these sites where PrP^{C} is also located. Our findings are compatible with any of these possible conversion sites.

Our EM experiments give a first hint on one possible way of how endocytosis of PrP^{Sc} in neuronal cells takes place, i.e., via clathrin-coated pits, which were identified by their morphology (Fig. 8A), although this observation needs further detailed investigation. To the best of our knowledge there are no publications demonstrating PrP^{Sc} internalisation via coated pits. PrP^{C} has also been reported to be endocytosed with clathrin-coated pits in neuronal cells (Shyng et al., 1995; Sunyach et al., 2003) and Jurkat cells (Langhorst et al., 2008). It is likely that PrP^{Sc} follows the same route as PrP^{C} and is internalised with clathrin-coated pits.

Moreover, PrP^{Sc} was detected to a small extent in early endosomes and late endosomes/lysosomes (Figs. 4, 8 and 9), while the bulk of PrP^{Sc} was located outside these compartments. Our data shown in the present paper go well beyond the status mirrored by the current literature: It had been well established that PrP^{Sc} resides in endosomes and lysosomes. For example, PrP^{Sc} was detected in LAMP-1-positive late endosomes/lysosomes and in LYAAT-positive lysosomes with IF (Pimpinelli et al., 2005; Kristiansen et al., 2007). Furthermore, EM analysis revealed PrP^{Sc} in acid phosphatase-positive compartments in cell culture (McKinley et al., 1991). In addition, PrP^{Sc} was observed in Rab5-positive early endosomes and cathepsin D- and B-positive compartments (Kovacs et al., 2007). Finally, in scrapie-infected mouse brain tissue or vCJD-infected brain tissue PrP^{Sc} was observed in late endosomes/lysosomes that were positive for hsp70, β-glucuronidase, ubiquitin conjugate, mannose-6-phosphate receptor, or an allegedly lysosome-specific lectin (Laszlo et al., 1992; Arnold et al., 1995; Grigoriev et al., 1999; Fournier et al., 2000). In our work, we combined PK digestion and GdnSCN denaturation in EM analyses to specifically demonstrate the presence of PrP^{Sc} in early endosomes and late endosomes/lysosomes. Such a strategy has never been reported before. Interestingly, PrP^{Sc} in LAMP-1- or LYAAT-positive organelles was much more abundant than in the present work although even in those publications PrP^{Sc} was found outside late endosomes/lysosomes (Pimpinelli et al., 2005; Kristiansen et al., 2007). This could be due to the mAB used. It is conceivable that pAB Limp2 detects other subpopulations of late endosomes/lysosomes than LAMP-1 or LYAAT ABs do. The signal intensity of EEA1 in the present work compared with the work of Pimpinelli et al. (2005) seemed to be comparable. In order to investigate the localisation site of PrP^{Sc}, apart from endosomes and lysosomes, IF localisation studies of PrP^{Sc} in ER, Golgi and nucleus were carried out, but these compartments were free from PrP^{Sc} (data not shown). Other investigators detected PrP^{Sc} in aggresomes upon proteasome inhibition (Kristiansen et al., 2005), which could explain why the majority of PrP^{Sc} is not associated with compartments although this would imply that the proteasome is intrinsically inhibited in the cell clone used here for scrapie infection. In our own experiments, however, we have never seen evidence for PrP^{Sc} localisation to aggresomes. Furthermore, the cytosol has been reported as a site for PrP^{Sc} localisation as described previously by colocalisation of PrP^{Sc} with hsc70 (Kristiansen et al., 2007). Finally, it is also conceivable that the majority of PrP^{Sc} is located in residual bodies/degraded lysosomes. These structures might well be negative for Limp2 and they might therefore have gone undetected in our study.

Release of PrP^{Sc} from infected ScN2a cells

In previous work on Jurkat T cells, PrP^{C} was detected in LBs, and exocytosis of LBs containing PrP^{C} could also be observed (Reuter et al., 2004). Therefore, we examined if PrP^{Sc} is present in LBs and if exocytosis of PrP^{Sc} also occurs via LBs (Fig. 10). In the absence of a LB-mediated exocytotic pathway in ScN2a cells, one common way to spread infectivity from cell to cell was observed via exosomes derived from multivesicular bodies that release their contents by fusion with the plasma membrane (Fig. 7). In addition, we observed 6H4 AB-labelled amorphous masses attached to ScN2a cells in a situation strongly suggesting exocytotic release. While occurrence of $PrP^{Sc}+PrP^{C}$ in multivesicular bodies is in line with previous reports on the occurrence of PrP^{Sc} in these organelles (Fevrier et al., 2004; Vella et al., 2007), we show for the first time the actual process of PrP release by exocytosis in a cellular context from a PrP^{Sc}-infected N2a cell line (Fig. 7). This supports

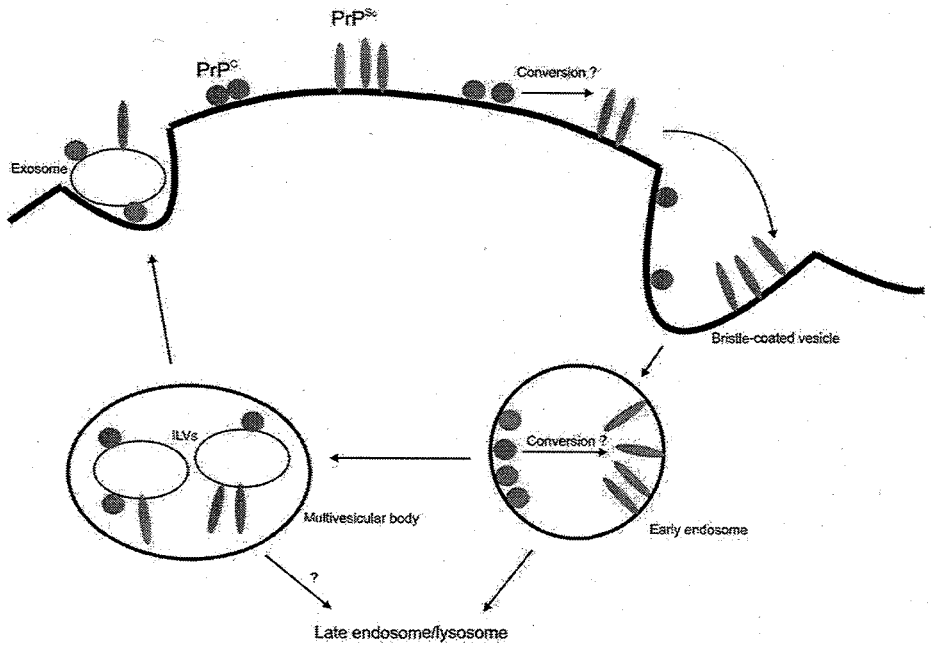

Fig. 11. Trafficking scheme of PrP proteins. This scheme summarises the findings on the infectious prion form, PrP^{Sc}, presented in this paper as well as complemented by other work cited in the text. It takes into account the pathways of the normal isoform, PrP^{C}, and the disease-associated isoform, PrP^{Sc}. Note that endocytotic pathways of PrP^{Sc} resemble those of PrP^{C}, but that currently we cannot exclude for PrP^{Sc} endocytotic mechanisms different from clathrin-coated pits and additional pathways of delivery to lysosomes. Question marks denote the putative conversion of PrP^{C} to PrP^{Sc} in these compartments. Multivesicular bodies are derived from early endosomes bearing intraluminal vesicles (ILVs) which are released in form of exosomes.

previous studies by Fevrier et al. (2004) showing multivesicular bodies labelled with anti-prion ABs inside PrP^{Sc}-infected cells from a rabbit kidney cell line and the occurrence of similar materials in the medium. All this supports a possible role in infection spreading.

Conclusion

In summary, we obtained new insights into the intracellular localisation of PrP^{Sc}, which has as yet been poorly understood. So far, the majority of immunolocalisation studies of PrP^{Sc} summarised in (Campana et al., 2005) have been performed without treatment to eliminate PrP^{C}, e.g., PK digestion. In contrast, we developed a method to perform PK digestion without losing cells, and a guanidine inactivation procedure without serious destruction of the (ultra-) structure in all EM analyses and in some IF experiments where the selective staining of PrP^{Sc} at the plasma membrane had to be guaranteed. We saw by IF that PrP^{Sc} is located at the plasma membrane and by EM that PrP^{Sc} is endocytosed via clathrin-coated pits. EM and IF analyses revealed that PrP^{Sc} is transported through early endosomes to late endosomes/lysosomes. The majority of PrP^{Sc}, however, was detected outside of these organelles and its localisation remains elusive. Possibly PrP^{Sc} localises to degraded lysosomes/residual bodies as these may preserve indigestible PrP^{Sc} better than any other components including organelle-specific ones. Such a situation has been shown to be present in rat liver (Plattner et al., 1975). As PrP^{Sc} is located at some of the same sites as established for PrP^{C} (cell membrane, early endosomes and late endosomes/lysosomes), the conversion process could take place at any of these sites. We observed release of PrP^{C} by exosomes derived from multivesicular bodies and, in addition, via unidentified amorphous materials, which represent potential mechanisms of intercellular spreading of prions. A summary of the trafficking pathways of PrP^{Sc} is depicted in Fig. 11.

Acknowledgements

We thank Prof. Sylvain Lehmann (Montpellier, France) for scrapie strain 22L, Prof. Walter Bodemer (Göttingen, Germany) for monoclonal antibody 12F10, and Dr. Alexander Raeber (Prionics, Zurich, Switzerland) for monoclonal antibody 6H4. We would like to thank Lauretta Nejedli, Sylvia Kolassa, Marianne Wiechers, and Katharina Hüttner for technical assistance, and Dr. Alexander Reuter for advice on lipid body isolation and staining. We gratefully acknowledge

funding by the EU Commission (FP6 NoE Neuroprion/ Priogen [grant to A. Bürkle]), Deutsche Forschungsgemeinschaft (TR-SFB 11 [grants to A. Bürkle and C.A.O. Stuermer]) and the TSE program by the Land Baden-Württemberg (grants to C.A.O. Stuermer and H. Plattner).

References

Armbruster, B.L., Carlemalm, E., Chiovetti, R., Garavito, R.M., Hobot, J.A., Kellenberger, E., Villiger, W., 1982. Specimen preparation for electron microscopy using low temperature embedding resins. J. Microsc. 126, 77–85.

Arnold, J.E., Tipler, C., Laszlo, L., Hope, J., Landon, M., Mayer, R.J., 1995. The abnormal isoform of the prion protein accumulates in late-endosome-like organelles in scrapie-infected mouse brain. J. Pathol. 176, 403–411.

Baron, G.S., Caughey, B., 2003. Effect of glycosylphosphatidylinositol anchor-dependent and -independent prion protein association with model raft membranes on conversion to the protease-resistant isoform. J. Biol. Chem. 278, 14883–14892.

Baron, G.S., Wehrly, K., Dorward, D.W., Chesebro, B., Caughey, B., 2002. Conversion of raft associated prion protein to the protease-resistant state requires insertion of PrP-res (PrP(Sc)) into contiguous membranes. EMBO J. 21, 1031–1040.

Beranger, F., Mange, A., Goud, B., Lehmann, S., 2002. Stimulation of PrP(C) retrograde transport toward the endoplasmic reticulum increases accumulation of PrP(Sc) in prion-infected cells. J. Biol. Chem. 277, 38972–38977.

Bernhard, W., Avrameas, S., 1971. Ultrastructural visualization of cellular carbohydrate components by means of concanavalin A. Exp. Cell Res. 64, 232–236.

Borchelt, D.R., Scott, M., Taraboulos, A., Stahl, N., Prusiner, S.B., 1990. Scrapie and cellular prion proteins differ in their kinetics of synthesis and topology in cultured cells. J. Cell Biol. 110, 743–752.

Borchelt, D.R., Taraboulos, A., Prusiner, S.B., 1992. Evidence for synthesis of scrapie prion proteins in the endocytic pathway. J. Biol. Chem. 267, 16188–16199.

Botto, L., Masserini, M., Cassetti, A., Palestini, P., 2004. Immunoseparation of Prion protein-enriched domains from other detergent-resistant membrane fractions, isolated from neuronal cells. FEBS Lett. 557, 143–147.

Campana, V., Sarnataro, D., Zurzolo, C., 2005. The highways and byways of prion protein trafficking. Trends Cell Biol. 15, 102–111.

Caughey, B., Baron, G.S., 2006. Prions and their partners in crime. Nature 443, 803–810.

Caughey, B., Raymond, G.J., 1991. The scrapie-associated form of PrP is made from a cell surface precursor that is both protease- and phospholipase-sensitive. J. Biol. Chem. 266, 18217–18223.

Caughey, B., Raymond, G.J., Ernst, D., Race, R.E., 1991. N-terminal truncation of the scrapie-associated form of PrP by lysosomal protease(s): implications regarding the site of conversion of PrP to the protease-resistant state. J. Virol. 65, 6597–6603.

Endo, T., Groth, D., Prusiner, S.B., Kobata, A., 1989. Diversity of oligosaccharide structures linked to asparagines of the scrapie prion protein. Biochemistry 28, 8380–8388.

Fevrier, B., Vilette, D., Archer, F., Loew, D., Faigle, W., Vidal, M., Laude, H., Raposo, G., 2004. Cells release prions in association with exosomes. Proc. Natl. Acad. Sci. USA 101, 9683–9688.

Fournier, J.G., Escaig-Haye, F., Grigoriev, V., 2000. Ultrastructural localization of prion proteins: physiological and pathological implications. Microsc. Res. Tech. 50, 76–88.

Frick, M., Bright, N.A., Riento, K., Bray, A., Merrified, C., Nichols, B.J., 2007. Coassembly of flotillins induces formation of membrane microdomains, membrane curvature, and vesicle budding. Curr. Biol. 17, 1151–1156.

Gilch, S., Winklhofer, K.F., Groschup, M.H., Nunziante, M., Lucassen, R., Spielhaupter, C., Muranyi, W., Riesner, D., Tatzelt, J., Schatzl, H.M., 2001. Intracellular re-routing of prion protein prevents propagation of PrP(Sc) and delays onset of prion disease. EMBO J. 20, 3957–3966.

Grigoriev, V., Escaig-Haye, F., Streichenberger, N., Kopp, N., Langeveld, J., Brown, P., Fournier, J.G., 1999. Submicroscopic immunodetection of PrP in the brain of a patient with a new-variant of Creutzfeldt-Jakob disease. Neurosci. Lett. 264, 57–60.

Hansen, S.H., Sandvig, K., van Deurs, B., 1993. Molecules internalized by clathrin-independent endocytosis are delivered to endosomes containing transferrin receptors. J. Cell Biol. 123, 89–97.

Herman, B., Albertini, D.F., 1982. The intracellular movement of endocytic vesicles in cultured granulosa cells. Cell Motil. 2, 583–597.

Hölscher, C., Delius, H., Bürkle, A., 1998. Overexpression of nonconvertible PrP^{c} delta114-121 in scrapie-infected mouse neuroblastoma cells leads to trans-dominant inhibition of wild-type PrP^{Sc} accumulation. J. Virol. 72, 1153–1159.

Kaneko, K., Vey, M., Scott, M., Pilkuhn, S., Cohen, F.E., Prusiner, S.B., 1997. COOH-terminal sequence of the cellular prion protein directs subcellular trafficking and controls conversion into the scrapie isoform. Proc. Natl. Acad. Sci. USA 94, 2333–2338.

Kovacs, G.G., Gelpi, E., Strobel, T., Ricken, G., Nyengaard, J.R., Bernheimer, H., Budka, H., 2007. Involvement of the endosomal–lysosomal system correlates with regional pathology in Creutzfeldt-Jakob disease. J. Neuropathol. Exp. Neurol. 66, 628–636.

Krasemann, S., Groschup, M.H., Harmeyer, S., Hunsmann, G., Bodemer, W., 1996. Generation of monoclonal antibodies against human prion proteins in $PrP^{0/0}$ mice. Mol. Med. 2, 725–734.

Kristiansen, M., Messenger, M.J., Klohn, P.C., Brandner, S., Wadsworth, J.D., Collinge, J., Tabrizi, S.J., 2005. Disease-related prion protein forms aggresomes in neuronal cells leading to caspase activation and apoptosis. J. Biol. Chem. 280, 38851–38861.

Kristiansen, M., Deriziotis, P., Dimcheff, D.E., Jackson, G.S., Ovaa, H., Naumann, H., Clarke, A.R., van Leeuwen, F.W., Menendez-Benito, V., Dantuma, N.P., Portis, J.L., Collinge, J., Tabrizi, S.J., 2007. Disease-associated prion

protein oligomers inhibit the 26S proteasome. Mol. Cell 26, 175–188.

Laine, J., Marc, M.E., Sy, M.S., Axelrad, H., 2001. Cellular and subcellular morphological localization of normal prion protein in rodent cerebellum. Eur. J. Neurosci. 14, 47–56.

Lang, D.M., Lommel, S., Jung, M., Ankerhold, R., Petrausch, B., Laessing, U., Wiechers, M.F., Plattner, H., Stuermer, C.A., 1998. Identification of reggie-1 and reggie-2 as plasmamembrane-associated proteins which cocluster with activated GPI-anchored cell adhesion molecules in non-caveolar micropatches in neurons. J. Neurobiol. 37, 502–523.

Langhorst, M.F., Reuter, A., Jaeger, F.A., Wippich, F.M., Luxenhofer, G., Plattner, H., Stuermer, C.A., 2008. Trafficking of the microdomain scaffolding protein reggie-1/flotillin-2. Eur. J. Cell Biol. 87, 211–226.

Laszlo, L., Lowe, J., Self, T., Kenward, N., Landon, M., McBride, T., Farquhar, C., McConnell, I., Brown, J., Hope, J., et al., 1992. Lysosomes as key organelles in the pathogenesis of prion encephalopathies. J. Pathol. 166, 333–341.

Liu, P., Ying, Y., Zhao, Y., Mundy, D.I., Zhu, M., Anderson, R.G., 2004. Chinese hamster ovary K2 cell lipid droplets appear to be metabolic organelles involved in membrane traffic. J. Biol. Chem. 279, 3787–3792.

Madore, N., Smith, K.L., Graham, C.H., Jen, A., Brady, K., Hall, S., Morris, R., 1999. Functionally different GPI proteins are organized in different domains on the neuronal surface. EMBO J. 18, 6917–6926.

Magalhaes, A.C., Silva, J.A., Lee, K.S., Martins, V.R., Prado, V.F., Ferguson, S.S., Gomez, M.V., Brentani, R.R., Prado, M.A., 2002. Endocytic intermediates involved with the intracellular trafficking of a fluorescent cellular prion protein. J. Biol. Chem. 277, 33311–33318.

Maher, P., Molday, R.S., 1981. Analysis of lectin-specific cell surface glycoprotein on neuroblastoma cells. Biochim. Biophys. Acta 647, 259–269.

Mange, A., Nishida, N., Milhavet, O., McMahon, H.E., Casanova, D., Lehmann, S., 2000. Amphotericin B inhibits the generation of the scrapie isoform of the prion protein in infected cultures. J. Virol. 74, 3135–3140.

Marella, M., Lehmann, S., Grassi, J., Chabry, J., 2002. Filipin prevents pathological prion protein accumulation by reducing endocytosis and inducing cellular PrP release. J. Biol. Chem. 277, 25457–25464.

McKinley, M.P., Taraboulos, A., Kenaga, L., Serban, D., Stieber, A., DeArmond, S.J., Prusiner, S.B., Gonatas, N., 1991. Ultrastructural localization of scrapie prion proteins in cytoplasmic vesicles of infected cultured cells. Lab. Invest. 65, 622–630.

Naslavsky, N., Stein, R., Yanai, A., Friedlander, G., Taraboulos, A., 1997. Characterization of detergent-insoluble complexes containing the cellular prion protein and its scrapie isoform. J. Biol. Chem. 272, 6324–6331.

Naslavsky, N., Shmeeda, H., Friedlander, G., Yanai, A., Futerman, A.H., Barenholz, Y., Taraboulos, A., 1999. Sphingolipid depletion increases formation of the scrapie prion protein in neuroblastoma cells infected with prions. J. Biol. Chem. 274, 20763–20771.

Nunziante, M., Gilch, S., Schatzl, H.M., 2003. Essential role of the prion protein N terminus in subcellular trafficking and half-life of cellular prion protein. J. Biol. Chem. 278, 3726–3734.

Paquet, S., Daude, N., Courageot, M.P., Chapuis, J., Laude, H., Vilette, D., 2007. PrPc does not mediate internalization of PrPSc but is required at an early stage for de novo prion infection of Rov cells. J. Virol. 81, 10786–10791.

Pauly, P.C., Harris, D.A., 1998. Copper stimulates endocytosis of the prion protein. J. Biol. Chem. 273, 33107–33110.

Pimpinelli, F., Lehmann, S., Maridonneau-Parini, I., 2005. The scrapie prion protein is present in flotillin-1-positive vesicles in central- but not peripheral-derived neuronal cell lines. Eur. J. Neurosci. 21, 2063–2072.

Plattner, H., Henning, R., Brauser, B., 1975. Formation of Triton WR 1339-filled rat liver lysosomes. II. Involvement of autophagy and of pre-existing lysosomes. Exp. Cell Res. 94, 377–391.

Prado, M.A., Alves-Silva, J., Magalhaes, A.C., Prado, V.F., Linden, R., Martins, V.R., Brentani, R.R., 2004. PrPc on the road: trafficking of the cellular prion protein. J. Neurochem. 88, 769–781.

Prusiner, S.B., 2001. Shattuck lecture – neurodegenerative diseases and prions. N. Engl. J. Med. 344, 1516–1526.

Renau-Piqueras, J., Miragall, F., Cervera, J., 1985. Distribution of concanavalin-A receptor sites on the surface of human resting T lymphocytes. A stereological study using concanavalin-A/colloidal-gold-labelled horseradish peroxidase. Histochemistry 82, 293–297.

Reuter, A., Binkle, U., Stuermer, C.A., Plattner, H., 2004. PrPc and reggies/flotillins are contained in and released via lipid-rich vesicles in Jurkat T cells. Cell. Mol. Life Sci. 61, 2092–2099.

Rudd, P.M., Endo, T., Colominas, C., Groth, D., Wheeler, S.F., Harvey, D.J., Wormald, M.R., Serban, H., Prusiner, S.B., Kobata, A., Dwek, R.A., 1999. Glycosylation differences between the normal and pathogenic prion protein isoforms. Proc. Natl. Acad. Sci. USA 96, 13044–13049.

Shyng, S.L., Huber, M.T., Harris, D.A., 1993. A prion protein cycles between the cell surface and an endocytic compartment in cultured neuroblastoma cells. J. Biol. Chem. 268, 15922–15928.

Shyng, S.L., Moulder, K.L., Lesko, A., Harris, D.A., 1995. The N-terminal domain of a glycolipid-anchored prion protein is essential for its endocytosis via clathrin-coated pits. J. Biol. Chem. 270, 14793–14800.

Stuermer, C.A., Lang, D.M., Kirsch, F., Wiechers, M., Deininger, S.O., Plattner, H., 2001. Glycosylphosphatidyl inositol-anchored proteins and fyn kinase assemble in noncaveolar plasma membrane microdomains defined by reggie-1 and -2. Mol. Biol. Cell 12, 3031–3045.

Stuermer, C.A., Langhorst, M.F., Wiechers, M.F., Legler, D.F., Von Hanwehr, S.H., Guse, A.H., Plattner, H., 2004. PrPc capping in T cells promotes its association with the lipid raft proteins reggie-1 and reggie-2 and leads to signal transduction. FASEB J. 18, 1731–1733.

Sunyach, C., Jen, A., Deng, J., Fitzgerald, K.T., Frobert, Y., Grassi, J., McCaffrey, M.W., Morris, R., 2003. The

mechanism of internalization of glycosylphosphatidylinositol-anchored prion protein. EMBO J. 22, 3591–3601.

Taraboulos, A., Serban, D., Prusiner, S.B., 1990. Scrapie prion proteins accumulate in the cytoplasm of persistently infected cultured cells. J. Cell Biol. 110, 2117–2132.

Taraboulos, A., Raeber, A.J., Borchelt, D.R., Serban, D., Prusiner, S.B., 1992. Synthesis and trafficking of prion proteins in cultured cells. Mol. Biol. Cell 3, 851–863.

Taraboulos, A., Scott, M., Semenov, A., Avrahami, D., Laszlo, L., Prusiner, S.B., 1995. Cholesterol depletion and modification of COOH-terminal targeting sequence of the prion protein inhibit formation of the scrapie isoform. J. Cell Biol. 129, 121–132.

Tatzelt, J., Schatzl, H.M., 2007. Molecular basis of cerebral neurodegeneration in prion diseases. FEBS J. 274, 606–611.

Taylor, D.R., Watt, N.T., Perera, W.S., Hooper, N.M., 2005. Assigning functions to distinct regions of the N-terminus of the prion protein that are involved in its copper-stimulated, clathrin-dependent endocytosis. J. Cell Sci. 118, 5141–5153.

Unterberger, U., Voigtlander, T., Budka, H., 2005. Pathogenesis of prion diseases. Acta Neuropathol. 109, 32–48.

Vella, L.J., Sharples, R.A., Lawson, V.A., Masters, C.L., Cappai, R., Hill, A.F., 2007. Packaging of prions into exosomes is associated with a novel pathway of PrP processing. J. Pathol. 211, 582–590.

Vey, M., Pilkuhn, S., Wille, H., Nixon, R., DeArmond, S.J., Smart, E.J., Anderson, R.G., Taraboulos, A., Prusiner, S.B., 1996. Subcellular colocalization of the cellular and scrapie prion proteins in caveolae-like membranous domains. Proc. Natl. Acad. Sci. USA 93, 14945–14949.

Wadsworth, J.D., Collinge, J., 2007. Update on human prion disease. Biochim. Biophys. Acta 1772, 598–609.

Weller, P.F., Monahan-Earley, R.A., Dvorak, H.F., Dvorak, A.M., 1991. Cytoplasmic lipid bodies of human eosinophils. Subcellular isolation and analysis of arachidonate incorporation. Am. J. Pathol. 138, 141–148.

Yi, J., Tang, X.M., 1999. The convergent point of the endocytic and autophagic pathways in Leydig cells. Cell Res. 9, 243–253.

Zhang, Y., Poirier, G.G., Burkle, A., 2002. In-situ analysis of cellular poly(ADP-ribose) production in scrapie-infected mouse neuroblastoma cells. Histochem. J. 34, 357–363.